Physical and numerical modeling of shear band formation

Modélisation physique et numérique de la formation des zones de cisaillement

R. Katzenbach & G. Bachmann
Technische Universität Darmstadt, Institute and Laboratory of Geotechnics, Germany
C. Gutberlet
GeoIngenieure Früchtenicht + Lehmann GmbH, Germany

ABSTRACT
Failure in soils is directly coupled to the formation of shear bands disconnecting the evolving failure body from the remaining soil continuum. For the scientific examination of shear band formation concerning earth pressure, base and slope failure several series of model tests are carried out at the Institute and Laboratory of Geotechnics of Technische Universität Darmstadt. The basics of these model tests and evaluation techniques are presented as well as a selection of test and numerical results.

RÉSUMÉ
La défaillance en sols va en pair avec la formation des zones de cisaillement qui détachent le naissant corps de défaillance du reste du continuum. Pour l'examination scientifique de la formation des zones de cas cisaillement à propos de la pression de terre, rupture du sol de fondation et de la pente, des séries d'essais de laboratoire sont exécutées à l'Institut et Laboratoire de Géotechnique à Technsiche Universität Darmstadt. Des techniques pour l'exécution et évaluation des tests sont présentées ainsi que certains des résultats des tests et simulations numériques.

Keywords : research and development, model experiments, shear band formation, numerical simulation

1 INTRODUCTION

Failure in soils is directly coupled to the formation of shear bands (e.g. Gudehus 1998, Gudehus 2004, Gudehus & Nübel 2004) disconnecting the evolving failure body from the remaining soil continuum, e.g. like it is observed within the passive earth pressure problem or during slope failures. Herein, the adequate determination of the relevant shear band is a prerequisite for the assessment of the stability of geotechnical structures. This is obvious regarding the proof of overall stability (slope stability) as it is carried out according to the given standards, e.g. Eurocode EC 7. Here, a limited number of systems with predefined shear bands and with shear parameters a priori reduced by a safety factor ("Fellenius' rule") are computed and the exploitation degree η is determined as a measure for the stability of the system. So it is evident that with this procedure the actually relevant shear band is not necessarily found (Katzenbach et al. 2008) because this one is not necessarily one of the considered systems.

A further aspect is the shear band formation in shifted soil that can only be mapped correctly with more sophisticated approaches, e.g. Finite Element Models. For the scientific examination of the shear band formation concerning earth pressure, base and slope failure several series of model tests are carried out at the Institute and Laboratory of Geotechnics of Technische Universität Darmstadt. The basics of these model tests and evaluation techniques are presented as well as a selection of test and numerical results.

2 MODEL TEST EVALUATION TECHNIQUES

The evaluation within the performed model test series comprises both conventional measuring of forces and displacements, e.g. by load cells and displacement transducers, as well as the measuring of the deformation fields in the soil continuum by means of the Particle Image Velocimetry (PIV, e.g. Nübel 2002, Pudasaini & Hutter 2006).

For the visualization of shear bands in the model tests the displacements measured by PIV are formed into the deviatoric strain as a scalar value. At first the strain tensor is computed from the displacements by

$$\varepsilon_{ij} = \frac{1}{2}\left(\frac{\delta u_i}{\delta x_j} + \frac{\delta u_j}{\delta x_i}\right) . \qquad (1)$$

From this the deviatoric strain tensor is determined by the following equation:

$$e_{ij} = \varepsilon_{ij} - \frac{\varepsilon_{kk}}{3} \cdot \delta_{ij} \qquad (2)$$

with e_{ij} as the deviatoric strain tensor, ε_{ij} as the tensor of strain, ε_{kk} the volumetric strain and δ_{ij} the Kronecker Delta. As a scalar magnitude for the shear strain is most useable, the deviatoric strain magnitude is computed as the Euclidian Norm of the deviatoric strain tensor according to

$$\varepsilon_p = \left\| e_{ij} \right\| = \sqrt{e_{ij} e_{ij}} \qquad (3)$$

with e_{ij} as the deviatoric strain tensor, ε_{ij} as the tensor of strain, ε_{kk} as the volumetric strain and δ_{ij} as the Kronecker Delta.

Displacements and strains have been accumulated throughout each test's development by means of an Euler-Lagrange-Transformation. This is necessary as the originally measured deformations are in an Eulerian description, which is orientated on the PIV measuring grid and not on the material like it is within a Lagrangerian description.

Proceedings of the 17th International Conference on Soil Mechanics and Geotechnical Engineering
M. Hamza et al. (Eds.)

doi:10.3233/978-1-60750-031-5-610

3 MODEL TESTS ON PASSIVE EARTH PRESSURE

The model tests on passive earth pressure are carried out in the model test rig displayed in Figure 1 (Gutberlet 2008). Earth pressure has been triggered by moving a wall into the soil continuum; in this publication we only regard the test with parallel wall movement.

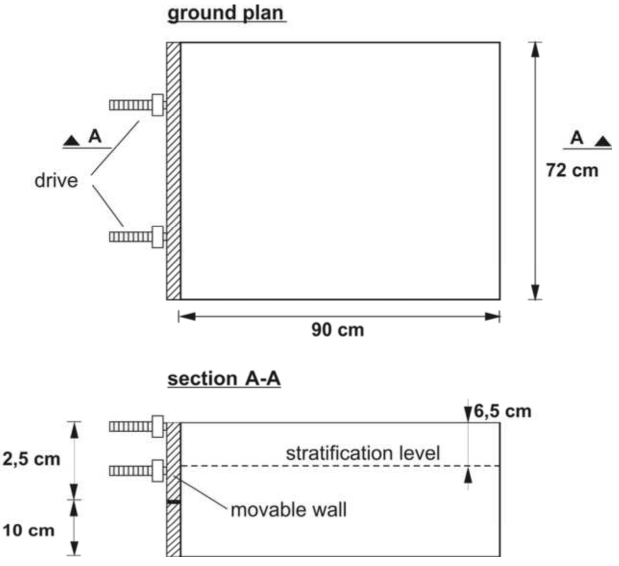

Figure 1. Ground plan and cross section through the model test rig

In Figure 2 two mobilisation curves, i.e. relationship between earth pressure E and wall displacement s, with „Darmstadt Sand“ (e.g. Festag 2003, Hettler & Gudehus 1985) with varying compaction (loose and very dense) can be observed. Obviously both systems exhibit completely differing behaviour: Whereas the earth pressure in the loosely filled sand continuously rises with wall displacement, the earth pressure in very dense sand soon reaches a peak value with subsequent decline of earth pressure down to some kind of critical level.

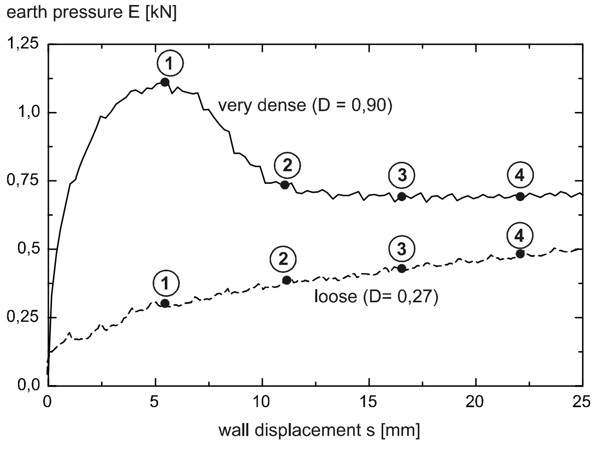

Figure 2. Earth pressure mobilization in loose and very dense Darmstadt Sand

For each four wall displacements states, which are marked by dots in Figure 2, we present the shear band formation in Figure 3 by means of shear strains accumulated by the above mentioned Euler-Lagrange-Transformation.

The evaluation of the deviatoric strain magnitude ε_p reveals for varying compactions distinct differences concerning the shear band formation (Figure 3). In the presented test with very dense Darmstadt Sand a shear band occurs with a quite small width whilst the remaining soil continuum does not exhibit relevant shear deformations. In the presented test with loose Darmstadt Sand the observable shear band is much more diffuse. Also, the curves of the shear band differ between both systems. In very dense sand, it has a obvious curvature whereas in loose sand it is very straight. The curvature of the shear band in very dense sand cannot be approached with the usual straight line according to Coulomb but rather it can be well described with approaches with curved shear bands, e.g. according to Terzaghi (1951) or Sokolovski (1960) / Pregl (2000).

It is remarkable that with reaching the earth pressure peak value in the test with very dense Darmstadt Sand (point 1 in Figure 2 at a wall displacement of s = 5.5 mm) no shear band is formed through the sand body. In this stage, only locally at the wall base shear deformations have been formed. A fully formed shear band is achieved not before reaching the critical level in the mobilisation curve. After this, the shear band does not alter in form, only the magnitude of shear strain is increasing.

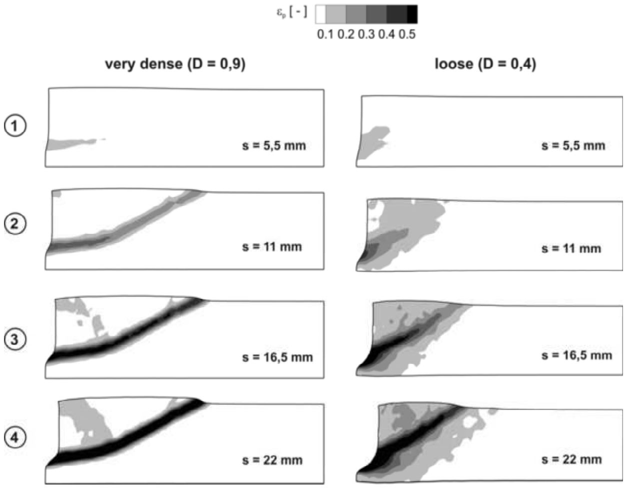

Figure 3. Evolution of shear band formation in model tests on passive earth pressure in loose and very dense Darmstadt Sand

With the installation of Darmstadt Sand with differing compaction states an effective stratification in the model tests can be achieved. The stratification border is in all tests about in the middle height of the moveable wall (see Figure 1). In Figure 4 the shear bands formed at large wall displacements (s ≈ 20 mm) are depicted. Evidently, at the stratification border a change in the shear band occurs. The characteristics of the shear bands (concentrated shear strains at very dense compaction and more diffuse at loose compaction) is coined by the compaction of the material at the wall base.

Concluding, it can be stated that the stratum at the wall base is coining the overall system behaviour, i.e. if there is very dense sand, the overall system behaves very similar to homogenous very dense sand and vice versa. This also concerns the mobilisation characteristics (Gutberlet 2008).

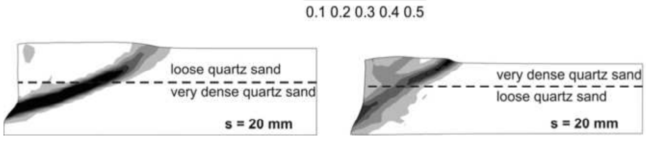

Figure 4. Shear band formation in model tests on passive earth pressure with stratified loose and very dense Darmstadt Sand

4 MODEL TESTS ON BASE AND SLOPE FAILURE

Model tests on base and slope failure have been carried out in the model test rig depicted in Figure 5. A model foundation has been forced into the installed soil continuum while the settlement of the foundation has been measured on all four corners and the applied force has been logged with load cells. The model foundation has been chosen quite long to approximate plane strain conditions. In this publication, we will confine on the model tests on slope failure. For all test results concerning base and slope failure, we refer to Bachmann (2009).

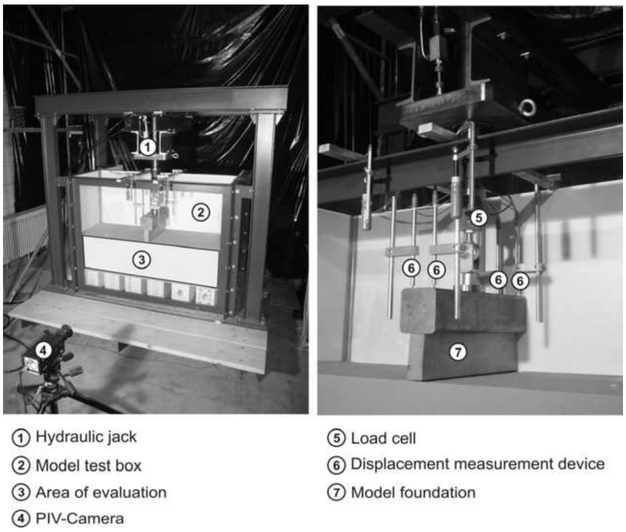

Figure 5. Model test setup for base and slope failure with model foundation

In Figure 6 the relationship between the bearing capacity factor N_b and the foundation settlement related to the foundation widths *s*/*b* is displayed for a selected slope failure test. The soil (also Darmstadt Sand) has been built in with very dense compaction. Analogously to the mobilisation curves of passive earth pressure in very dense sand, the bearing capacity declines after reaching a peak value and eventually it reaches a critical level.

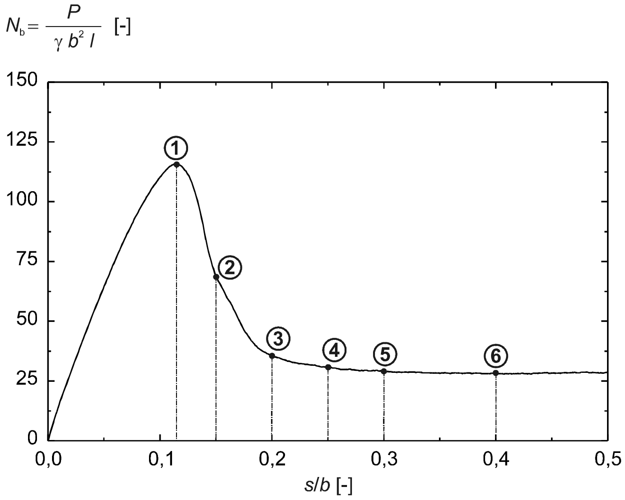

Figure 6. Mobilisation of bearing capacity factor N_b over foundation settlement related to foundation widths *s*/*b* during slope failure test

So we regard in Figure 7 for each displacement state of the foundation which are marked in Figure 6 with dots the according shear deformations: Unlike at the passive earth pressure tests, distinct shear strains Comparable to the earth pressure tests the shear band starts forming after reaching the peak value in the mobilisation curve of the bearing capacity (point 1). Afterwards the shear band formation progresses, until at point 3 after reaching the critical stage it is completely formed. Further settlements do not cause further changes in the shear band, but rather in the magnitude of shear strains.

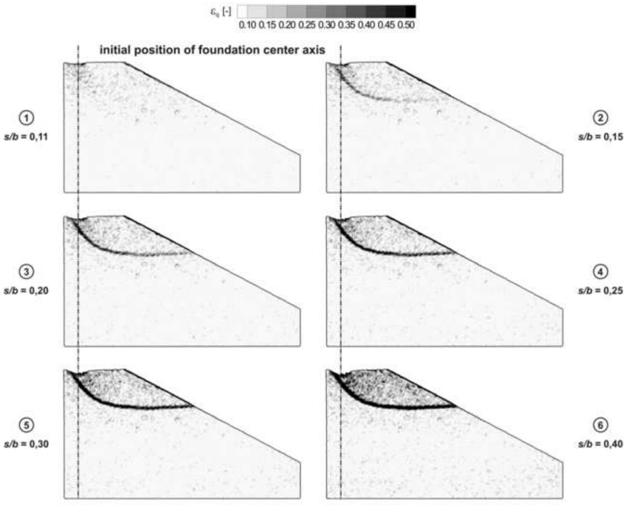

Figure 7. Evolution of shear band formation in model test on slope failure in very dense Darmstadt Sand

5 NUMERICAL INVESTIGATIONS

The model test series are supplemented by numerical investigation with the Finite Element Method. For the description of behaviour of sand, especially under small stress conditions, the hypoplastic constitutive law according to Gudehus (1995) and von Wolffersdorff (1996) is appropriate. With these numerical investigations, it is possible to model both the force mobilisations and the shear band formation; it moreover enables the determination of further field magnitudes like stress or void ratio. Eventually, with a validated numerical test set-up parameter studies can be carried out that are not easily performed under model test conditions.

For Darmstadt Sand we apply the parameter set as it is given in Table 1.

Table 1. Hypoplastic parameters for Darmstadt Sand

Magnitude	**Symbol / Dimension**	**Value**
Critical angle of friction	φ_c [°]	32,3
Hardness	h_S [kPa]	10^7
Exponent	n [-]	0,25
Void ratio at densest compaction	e_{d0} [-]	0,48
Void ratio in critical state	e_{c0} [-]	0,80
Void ratio in loosest compaction	e_{i0} [-]	1,00
Exponent	α [-]	0,15
Exponent	β [-]	1,5

A numerical test set-up (Katzenbach et al. 2005) is validated by means of numerical back-analysis of the model tests. In Figure 8 the mobilisation curve of a passive earth pressure test with very dense sand is compared to the curves according a numerical computation with a hypoplastic constitutive law and a computation with the Mohr-Coulomb-Model.

With this validated numerical test set-up, further evaluations of magnitudes can be performed. In Figure 9, earth pressure stresses on the moveable wall are depicted. These stresses could not be determined due to the small model test dimensions. It can be seen that there is a decline of earth pressure stresses at the wall base after trespassing the earth pressure peak value (at a displacement of s = 4 mm) indicating the influence of the soil at the wall base coining the overall system behaviour.

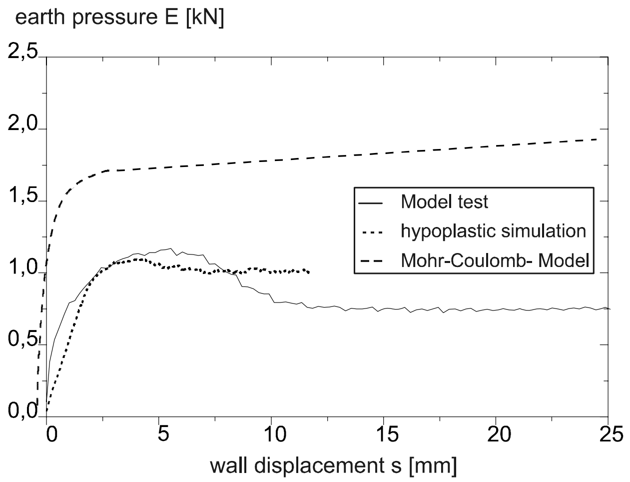

Figure 8. Mobilisation curve from passive earth pressure test with very dense Darmstadt Sand compared to curves of numerical computations

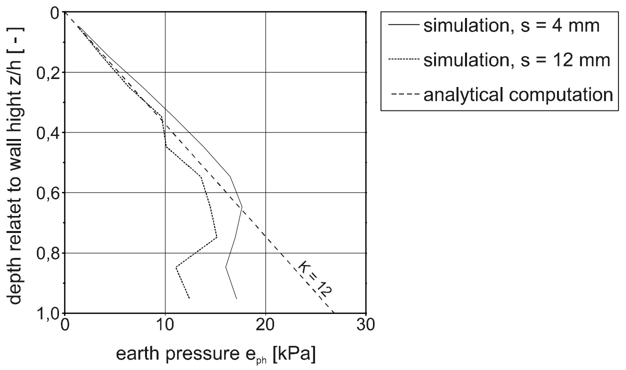

Figure 9. Computed passive earth pressure stresses for two stages (s = 4 mm: earth pressure maximum according to Figure 8; s = 12 mm: critical level)

6 SUMMARY AND CONCLUSION

The shear band formation – an important input in stability computations – is a object of actual research in Geotechnical Engineering. At the Institute and Laboratory of Geotechnics at Technische Universität Darmstadt, model tests and numerical studies on the formation of shear bands in homogenous and stratified soil are performed. In this paper, the general technique of execution and evaluation of model test on passive earth pressure and slope failure have been presented and results are discussed. Also numerical analyses of the model tests on passive earth pressure using hypoplastic material behaviour are presented.

REFERENCES

Bachmann, G. (2009). Bruchentwicklung bei Grund- und Böschungsbruch - Experimente und Numerik. Mitteilungen des Institutes und der Versuchsanstalt für Geotechnik der Technischen Universität Darmstadt, Heft 81

Festag, G. (2003). Experimentelle und numerische Untersuchungen zum Verhalten von granularen Materialien unter zyklischer Beanspruchung. Mitteilungen des Institutes und der Versuchsanstalt für Geotechnik der Technischen Universität Darmstadt, Heft 66

Gudehus, G. (1995). A comprehensive constitutive equation for granular materials. Soils and Foundations, Jap. Soc. Soil. Mech.

Gudehus, G. (1998). Shear localization in simple grain skeletons with polar effects. Proc. 4th International Workshop on Localization and Bifurcation Theory for Soils and Rocks, Gifu/Japan 1997, 3-10.

Gudehus, G. (2004). Hypoplastic shear localisation in psammoids and peloids. Proceedings of 2nd International Symposium on Continuous and Discontinuous Modelling of Cohesive-Frictional Materials – CDM 2004, Stuttgart, S. 411-421, A.A. Balkema Publishers, Leiden

Gudehus, G., Nübel, K. (2004). Evolution of Shear Bands in Sand. Geotechnique, 52/3, S. 187-201

Gutberlet, C. (2008). Erdwiderstand in homogenem und geschichtetem Baugrund – Experimente und Numerik. Mitteilungen des Institutes und der Versuchsanstalt für Geotechnik der Technischen Universität Darmstadt, Heft 78

Hettler, A., Gudehus, G. (1985). A pressure-dependant correction for displacement results from 1g model tests with sand. Géotechnique 35, 497-510

Katzenbach, R., Bachmann, G., Gutberlet, C. (2005) Pile-Soil-Wall-Interaction during the construction process of deep excavation pits. Proc. 16th International Conference on Soil Mechanics and Geotechnical Engineering, Osaka, 1501-1504

Katzenbach, R., Gutberlet, C.,. Bachmann, G. (2008). Progressiver Bruch und seine Auswirkungen auf die Standsicherheit geotechnischer Systeme. Mitteilungen des Institutes und der Versuchsanstalt für Geotechnik der Technischen Universität Darmstadt, Heft 79, 53-72

Pregel, O. (2000). Bemessung von Stützbauwerken; Handbuch der Geotechnik, Band 16; Institut für Geotechnik, Universität für Bodenkultur Wien

Pudasaini, S.P., Hutter, K. (2006). Avalanche dynamics. Springer Verlag, Berlin

Nübel, K. (2002). Experimental and numerical investigation of shear localization in granular material. Veröffentlichungen des Institutes für Bodenmechanik und Felsmechanik der Universität Fridericiana in Karlsruhe, Heft 159

Sokolovski, V.V. (1960). Statics of soil media. Butterworth, London.

von Terzaghi, K. (1951). Theoretical Soil Mechanics. Wiley & Sons, Newe York, 6. Auflage

von Wolffersdorff, P.-A. (1996). A hypoplastic relation for granular materials with a predefined limit state surface. Mechanics of Cohesive-Frictional Materials, 1:251-271